Journal of Materials Science and Chemical Engineering, 2025, 13(10), 85-97
https://www.scirp.org/journal/msce
ISSN Online: 2327-6053
ISSN Print: 2327-6045

Mineralogical and Physico-Chemical Characterization of Raw Iron Ore from Bandjéli in Bassar Prefecture in Northern Togo

Messan Justin Kessouagni[1,2], Moursalou Koriko[1*], Koffi Fiaty[2], Catherine Charcosset[2], Xavier Jaurand[3], Arnaud Brioude[4], Gado Tchangbedji[1]

[1]Laboratoire de Gestion Traitement et Valorisation des Déchets (GTVD), Université de Lomé, Faculté des Sciences, Lomé, Togo
[2]Université Claude Bernard Lyon 1, Laboratoire d'Automatique, de Génie des Procédés et de Génie Pharmaceutiques (LAGEPP), Bât CPE-Lyon, UMR CNRS 5007, Villeurbanne, France
[3]Université Claude Bernard Lyon 1, Centre technologique des Microstructures, Bât DARWIN B, 5 rue Raphael Dubois, Villeurbanne Cedex, France
[4]Université Claude Bernard Lyon 1, Laboratoire des Matériaux et Interfaces (LMI), Bât Chevreul, UMR CNRS 5615, Villeurbanne Cedex, France
Email: *moursalou7@hotmail.com, mkoriko@univ-lome.tg

How to cite this paper: Kessouagni, M.J., Koriko, M., Fiaty, K., Charcosset, C., Jaurand, X., Brioude. A. and Tchangbedji, G. (2025) Mineralogical and Physico-Chemical Characterization of Raw Iron Ore from Bandjéli in Bassar Prefecture in Northern Togo. *Journal of Materials Science and Chemical Engineering*, **13**, 85-97.
https://doi.org/10.4236/msce.2025.1310005

Received: September 23, 2025
Accepted: October 28, 2025
Published: October 31, 2025

Abstract

In order to contribute to the optimisation of industrial and domestic wastewater treatment using plasma-based methods coupled with photo-Fenton processes catalysed by natural iron ores extracted from soils, the physicochemical and mineralogical characterizations of these minerals were investigated. The characterizations were carried out by X-ray diffraction (XRD), scanning electron microscopy combined with energy dispersive spectroscopy (SEM-EDX), X-ray fluorescence spectroscopy (XRF), Fourier transform infrared spectroscopy (FTIR) and thermogravimetric analysis (TGA). X-ray fluorescence (XRF) analysis indicates a predominant presence of hematite, characterized by a high iron content of 95.84%. The sample exhibits a low concentration of gangue minerals, with 4.19% SiO_2 and 1.45% Al_2O_3, and low levels of undesirable elements (0.15% S; 0.04% P; 0.06% Mn; 0.02% Cr; 0.01% Sr). These compositional data serve as a critical baseline for advanced investigations in materials chemistry, process optimization in extractive metallurgy, and the development of environmentally sustainable resource management strategies.

Keywords

Characterization, Iron Ore, Bandjéli, Industrial Valorization

1. Introduction

Physicochemical and mineralogical characterization of iron ore represents a fundamental challenge for both the global steel industry and the development of advanced materials [1]. In particular, accurate characterization of the mineralogical and physicochemical properties of ores plays a key role in optimizing processes and assessing their environmental impact [2] [3]. Research conducted on various deposits, notably in Algeria and Uganda, has highlighted the value of a multi-analytical approach combining X-ray diffraction (XRD), X-ray fluorescence spectroscopy (XRF), scanning electron microscopy combined with energy dispersive spectroscopy (SEM-EDX) and thermal analysis technique (TGA).

All these techniques allow for a better understanding of the mineral composition, microstructure and chemical properties of ores [4] [5]. These data are essential for optimizing metallurgical performance and for forecasting and mitigating the environmental footprint associated with resource extraction.

Furthermore, earlier research has demonstrated that the presence of various mineral phases, including hematite, magnetite, goethite, and kaolinite has a direct impact on ore reactivity and the treatment processes applied to it [2] [6]. Evaluating the concentrations of trace elements (Si, Al, P, S, etc.) is a key factor in determining the suitability of the ore for applications in steelmaking and other industrial sectors, as well as in anticipating potential environmental risks [3] [5]. While extensive research has been conducted on major deposits across Africa and other regions [4] [8] [9], there is still a notable gap in recent, comprehensive, and especially quantitative and analytical studies focused on the Bandjéli raw ore in Togo.

The scientific literature concerning the iron ore of Bandjéli, a commune in the prefecture of Bassar (Northern Togo), is well documented in terms of archaeological, historical, metallographic, metallurgical, and mineralogical aspects, as well as its extraction and transformation into iron. Among the dedicated studies, the research conducted by P. de Barros *et al.* [10] notably focused on ironworking in Bassar, the detailed production and transformation chain of the ore into iron, and the chemical analysis of the Bandjéli and Bassar deposits. Furthermore, international and interdisciplinarity projects such as SidérENT (Ironworking and Environment in Togo, 2014-2018) have highlighted the interactions between the environment, society, and the traditional iron industry in Bassar, while emphasizing the richness and specificity of the local ore [11].

However, despite this abundant documentation on the history and ancient ironworking related to Togolese iron (dating, archaeology, metallurgy), the lack of comprehensive modern analytical data remains a significant obstacle to the scientific and industrial valorization of this strategic resource. It is in this context that we have undertaken a comprehensive characterization study of the Bandjéli iron ore deposit, located in the Bassar region of Togo, with the aim of obtaining and providing a set of relevant data that can facilitate future industrial applications and the development of these deposits. This dataset will include characterization techniques such as XRD, TGA, SEM-EDX, and FTIR.

2. Materials and Methods

2.1. Materials

Bassar Prefecture is situated within Zone IV of the ecological map of Togo (**Figure 1**). It encompasses the canton of Bandjéli, located approximately 36 km west of the town of Bassar, at geographic coordinates 09˚42'19" N latitude and 0˚62'43" E longitude. Traditional ironworking has been practiced in the area for several decades using artisanal methods. The town of Bassar is located at 395 km from Lomé, the capital city. The Bandjéli iron ore deposit was exploited by MM Mining SA between 2008 and 2014 [11]. Mining operations extended over an estimated 3708 km^2 within the most external structural unit of the Pan-African Dahomeyides fold belt, named Buem in the area of Bassar in Togo, and approximately 11,621 km^2 within the Atakora structural unit. The iron ore reserves, estimated at 500 million metric tons, are found at depth ranging from 10 to 30 m from the ground surface [11].

A one-week sampling campaign was carried out at the Bandjéli processing site to collect raw iron ore samples. The sampling strategy followed a systematic plan consisting of taking sub-samples at regular intervals from all ore stocks, in order to ensure homogeneous coverage of the different storage areas. Each sample was composed by combining several sub-samples taken from strategic points to ensure the overall representativeness of the mineral resources present. This approach provides a reliable and unbiased estimate of the average mineralogical and chemical composition of the ores on the site. Post-collection, samples were washed with distilled water for one hour, dried, ground in a mortar with an agate pestle, and sieved using an AS 400-Retsch automatic vibrating sieve to obtain powders with particle sizes less than or equal to 50 µm. The prepared samples were stored at room temperature in polypropylene containers until analysis.

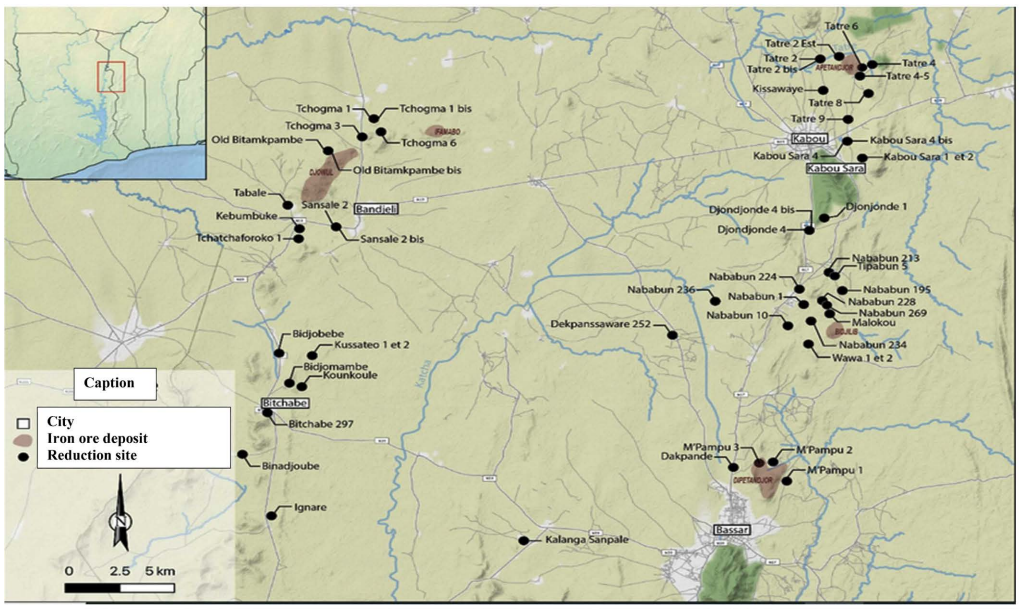

Figure 1. Location of the Bassar region (North Togo) [10].

2.2. Characterization Methods

A set of characterization techniques, including XRF, XRD, FTIR, SEM-EDX, TGA and TDA was employed to assess the physicochemical properties of the stockpiled raw iron ore samples.

X-Ray Fluorescence (XRF) was used to determine their chemical composition. The analyses were performed in Analytical Chemistry Laboratory (CPE Lyon) using an S2 PUMA spectrometer, the results were processed with XRF SPECTRA ELEMENTS software.

In order to evaluate the thermal behaviour of the ores, thermogravimetric analysis (TGA) and differential thermal analysis (DTA) were carried out using a NETZSCH TG 209 F122-10-210-K device, equipped with a furnace capable of reaching temperatures up to 1200 ˚C. Approximately 10 mg of sample wase heated in an aluminium crucible from 25 ˚C to 1000 ˚C at a heating rate of 10 ˚C/min under a nitrogen gas flow to limit oxidation reactions. The evolution of mass loss as a function of temperature was obtained using the NETZSCH PROTEUS thermal analysis software

Fourier Transform Infrared (FTIR) spectroscopy was also conducted to identify the functional groups present in the samples. The device used for the measurements is a Nicolet IS50 FTIR spectrometer from Thermo Fisher Scientific. IR Spectra were collected in absorbance mode over the region 400 - 4000 cm^{-1}. OMNIC SPECTRA 9 software was then used to analyze specific absorption peaks and identify the molecular bonds present.

For X-Ray Diffraction (XRD) analysis, prior to measurements, samples were placed in the poly(methyl methacrylate) sample holders, pressed with a polish glass slide to obtain a uniform surface, then fixed to the sample holder support of the Bruker D8 Advance diffractometer. Measurements were performed in Bragg-Brentano geometry with an equipment operating at 40 kV and 40 mA, using a Cu Kα radiation source ($\lambda = 1.5406$ Å). Analyses were monitored in real time on a computer connected to the diffractometer. Results were converted using File change software for easy processing. Minerals were identified using the standard DIFFAC.EVA software with a database from the International Centre for Diffraction (ICDD). All the XRD analyses were conducted at the Henri Longchambon Diffractometry Centre at University Claude Bernard Lyon-1 (CDHL) in Lyon, France.

In order to observe the morphology and surface structure, including pores and defects, a scanning electron microscopy (SEM) analysis was performed. This analysis was coupled with energy-dispersive X-ray spectroscopy (EDX) to identify the elemental and chemical composition of the raw ore. For the SEM-EDX sample preparation, the samples were introduced into a high-vacuum carbon coating device (BAL-TEC MED 020 High Vacuum), in order to deposit a 10 nm thick carbon layer on the surface of the samples, to avoid charge effects during SEM-EDX analysis. After carbon evaporation, the samples were transferred to a ZEISS MERLIN COMPACT VP scanning electron microscope for SEM and EDX analyses. The

resulting images were visualized using SMARTSEM Control software for Zeiss SEM, while the EDX data were processed using OXFORD AZtec software.

3. Results and Discussion

3.1. Chemical Analysis by XRF

X-ray fluorescence (XRF) analysis of the sample (Table 1) reveals a composition consisting mainly of hematite (93.45%), accompanied by low levels of silica (4.19%) and alumina (1.45%). Detailed elemental analysis (Table 2) reveals the predominant presence of iron (Fe 95.84%), followed by silicon (2.54%), aluminum (0.98%), and then smaller quantities of magnesium (Mg 0.20%), sulfur (0.15%), and other minor elements such as titanium, chlorine, manganese, phosphorus, chromium, vanadium, and strontium with concentrations lower than 0.1%. This high hematite content and low proportion of secondary elements attest to the high purity of Bandjéli ore, making it particularly suitable for applications in advanced oxidation processes. Indeed, the direct use of this ore as a source of iron in processes such as Fenton, photo-Fenton, or photocatalysis in sunlight shows promise for the degradation of emerging organic pollutants, which are often resistant to conventional or biological treatments. Unlike the conventional use of commercial iron salts, the integration of natural ore significantly reduces operating costs, which favors the extension of these processes to an industrial scale. In addition, hematite has a broad absorption range in the visible spectrum, facilitating the use of sunlight as an activation source and advantageously replacing expensive UVA/UVB lamps, whose use currently limits the widespread deployment of these technologies. Finally, the presence of trace elements in the ore does not hinder its application: it has been demonstrated that these impurities can be effectively removed by a simple preliminary acid or thermal treatment, ensuring compliance with discharge standards for undesirable elements during the recovery of Bandjéli ore for industrial wastewater treatment [12].

Table 1. Chemical oxide composition of crude iron ore measured by XRF.

Oxide	Fe_2O_3	SiO_2	Al_2O_3	MgO	SO_3	TiO_2	MnO	P_2O_5	Cr_2O_3	V_2O_5	Cl	SrO
Wt (%)	93 .45	4.19	1.45	0.30	0.29	0.10	0.05	0.06	0.02	0.05	0.05	0.01

Table 2. Elemental chemical composition of crude iron ore measured by XRF.

Element	Fe	Si	Al	Mg	S	Ti	Cl	Mn	P	Cr	V	Sr
Wt (%)	95.84	2.54	0. 98	0.20	0.15	0.08	0.07	0.06	0.04	0.02	0.01	0.01

3.2. Thermal Behavior

A study of the thermal gravimetry analysis shown in Figure 2 reveals stages with no loss of mass, indicating a certain stability of the ore in the temperature range of our analysis. A very small mass loss of 0.98% occurred between 30˚C and

1000˚C, due to material reduction. The total mass loss is 0.98%. This mass decrease corresponds probably to the partial deoxygenation of the hematite present in the ore. The small amount of mass loss is consistent with the presence of minor amounts of alumina and quartz, which are thermally stable within this temperature range.

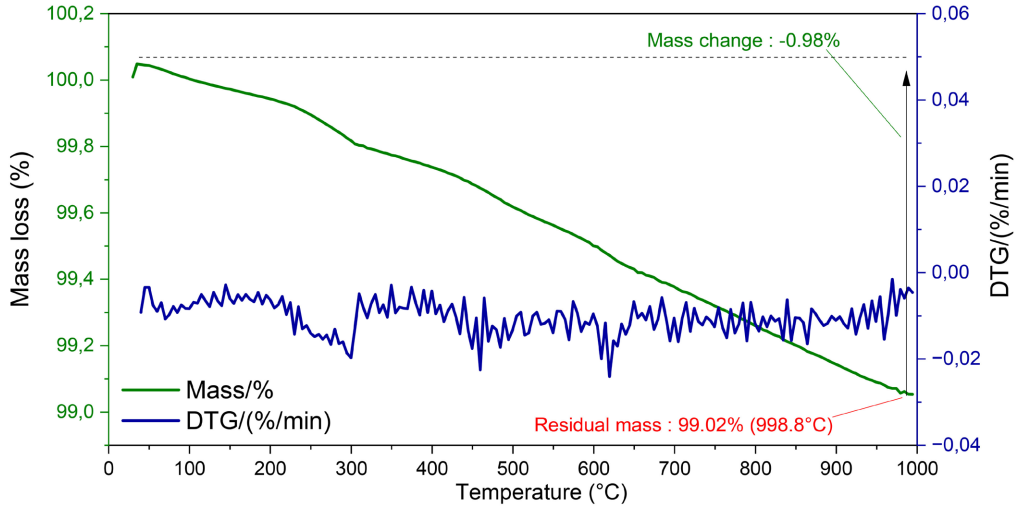

Figure 2. Thermal behavior of Bandjéli crude iron ore.

3.3. X-Ray Diffraction Analysis of Raw Iron Ore

The X-ray diffraction spectra of the crude sample is shown in **Figure 3**. The spectral analysis of the ore shows a majority of diffraction lines attributed to hematite 81.3% and quartz 18.7%. These results confirm those obtained during chemical analysis, which show a high proportion of hematite. Nevertheless, although this content attributed to the crystalline hematite phase is high, it remains lower than that obtained from the XRF analysis. This difference can be explained by the inherent limitations of the XRD method, which only quantifies detectable crystalline phases. Some of the iron may be present in amorphous or non-crystalline phases, which are not identifiable by X-ray diffraction but are detected by XRF. The XRF technique measures overall elemental composition. Furthermore, XRD quantification is subject to greater uncertainties related to the relative peak intensities and the modeling of multiple phases, whereas XRF provides a total measurement, including all mineral forms of iron. This complementarity justifies the observed discrepancy between the two techniques.

3.4. SEM-EDX Results

SEM analysis was employed to characterize the material morphology. The backscattered electron (BSE) imaging technique was used to differentiate the mineral phases present in the samples. This method relies on the intensity contrast related to the average atomic number (Z) of the analyzed phases: areas rich in

heavy elements, scatter backscattered electrons more effectively and therefore appear brighter in the images. Conversely, phases composed of lighter elements, exhibit lower contrast and appear darker. This differentiation based on atomic contrast allows for clear visual identification and provides complementary qualitative information to the chemical characterization by EDX. The SEM micrographs of the ore, shown in **Figure 4**, reveal the presence of two distinct phases. On one hand, hematite appears with two different populations of particles: smooth and angular grains ranging in size from approximately 5 to 10 µm, and small grains (less than 1 µm) that are more or less agglomerated and cover the entire surface. In **Figure 4(D)**, Hematite can be recognizable by its higher contrast with back-scattered electron SEM imaging. On the other hand, quartz-rich grains are approximately 10 to 20 µm in size and have a darker contrast with back-scattered electron SEM imaging.

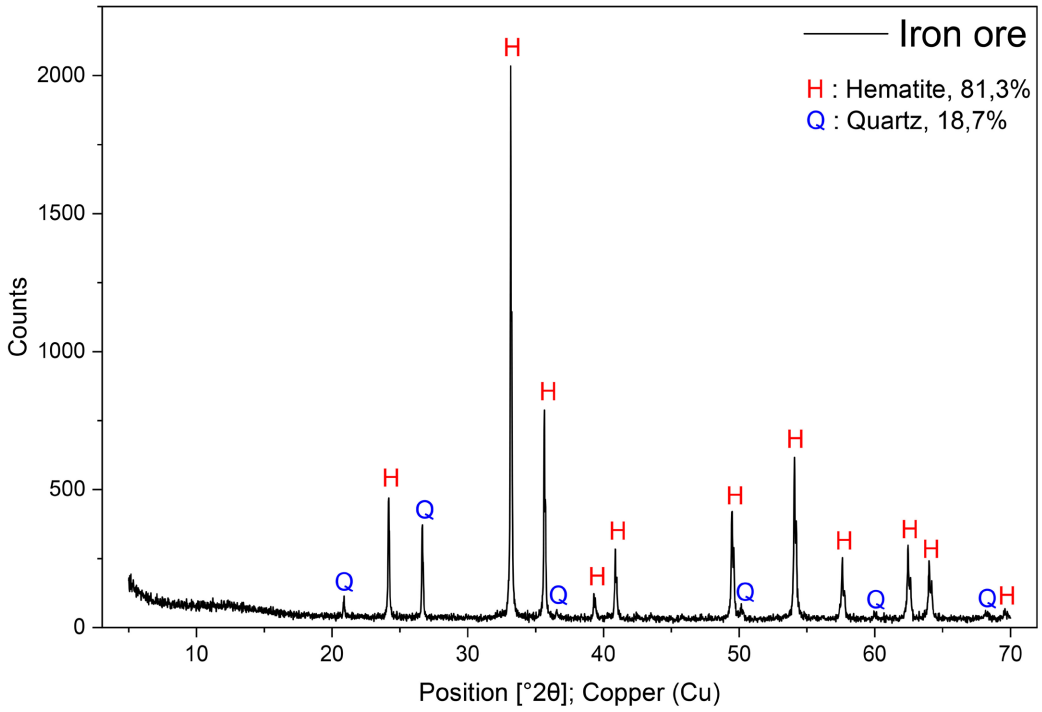

Figure 3. XRD spectrum of Bandjéli crude iron ore.

These results are consistent with the X-ray diffraction (XRD) analysis performed on natural iron ore. **Table 3** shows, using EDX, an overall composition dominated by Fe_2O_3 at 82%, indicating a mainly ferric ore. Spot analyses reveal high iron homogeneity in two areas (spectra 2 and spectra 3), while other areas (spectra 4 and spectra 5) show a high presence of SiO_2 (44% - 46%), suggesting localized siliceous inclusions. This variability reflects a heterogeneous microstructure, which is important to consider for the catalytic or environmental applications of this natural material. **Figure 5** shows EDX elemental mappings of raw iron ore. Spatial distribution of elements is shown on **Figures 5(b)-(e)** respec-

tively for oxygen, iron, silicon, and aluminium in the ore. Figure 5(f) shows the layered image of Al, Fe and Si elemental mappings. These analyses also confirm the presence of 2 main minerals. Figure 6 presents the quantitative analyses of the raw iron ore from Bandjéli performed by EDX. To investigate the sample's composition, measurements were taken at various locations corresponding to spectrum positions 2 to 5, as shown in Figure 6(a). The global spectrum analysis is displayed in Figure 6(b), while the spectra from points 2 to 5 are shown in Figure 6(c) and Figure 6(d). The quantitative results obtained are summarized in Table 3. Its can be seen that for the global spectrum a total oxide content of about 82% for hematite, 11% for silica, and 7% for alumina. This result is consistent with those obtained by XRD and XRF analyses regarding the significant amount of hematite present in the sample. Nevertheless, a heterogeneity in the distribution of the sample's constituent elements can be observed, as indicated by the spectral analyses from positions 2 to 5. Spectra 2 and 3, in particular, a hematite-rich grains are composed of about 95% - 96% for hematite, 1% - 2% for silica, 2% - 4% for alumina (Figure 6(c)) whereas spectra 4 and 5 a quartz-rich grains show a more heterogeneous composition with lower hematite concentrations are composed of about 52% - 53% for hematite, 44% - 46% for silica, 2% - 3% for alumina (Figure 6(d)).

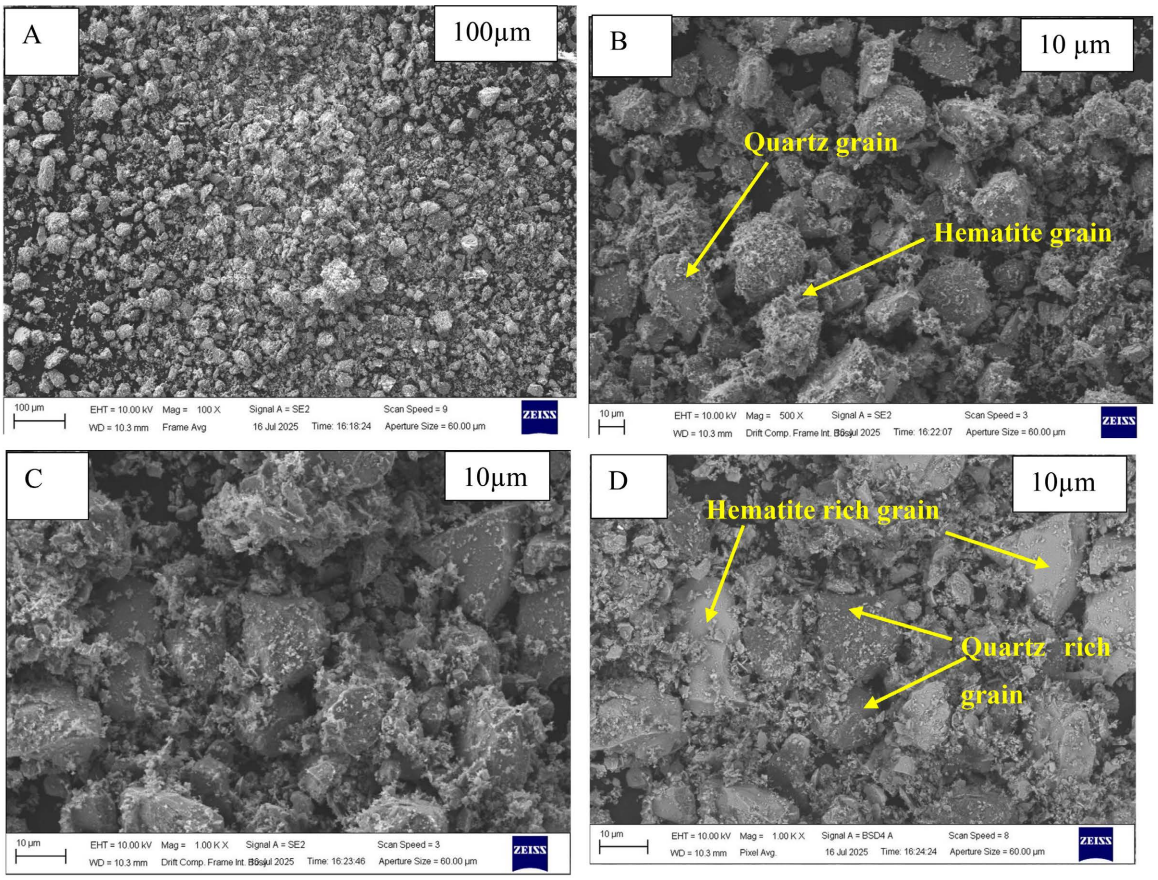

Figure 4. SEM images of Bandjéli raw iron ore for particle size fractions 100 µm (A) and 10 µm (B, C, D). (C) and (D) represent the same area and show respectively the topography with secondary electrons and the Z contrast with backscattered electrons.

Table 3. Elemental chemical composition in oxides, measured by EDX, for the entire sample and for the specific points corresponding to spectra 2 to 5.

Oxide	Global (%)	Spectrum 2 (%)	Spectrum 3 (%)	Spectrum 4 (%)	Spectrum 5 (%)
Al_2O_3	7	4	2	2	3
SiO_2	11	1	2	46	44
Fe_2O_3	82	95	96	52	53
Total	100	100	100	100	100

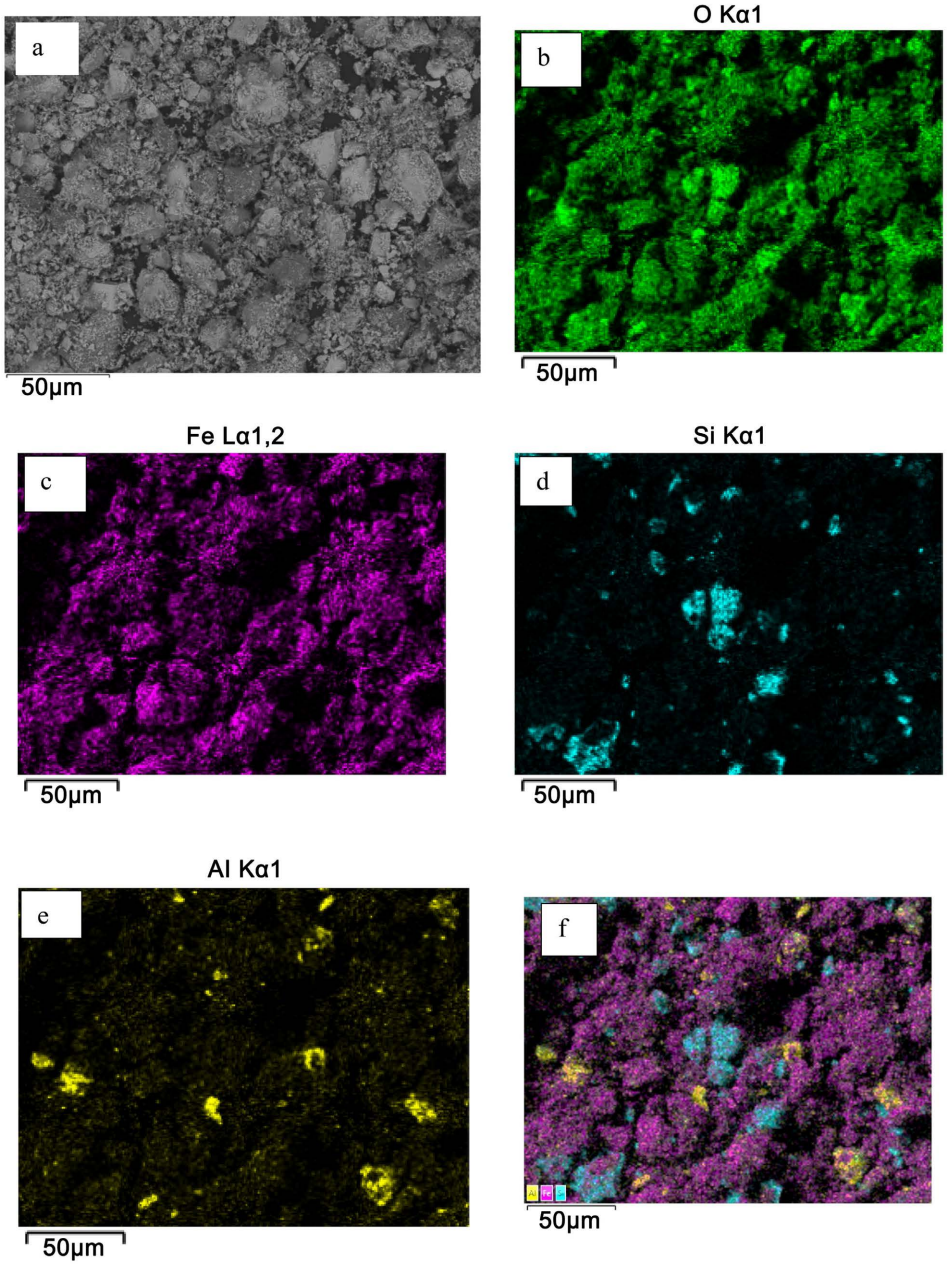

Figure 5. SEM images of raw iron ore from Bandjéli (a), elemental mappings of (b) oxygen, (c) iron, (d) silica, (e) aluminum, and a superimposition of the four elements (f).

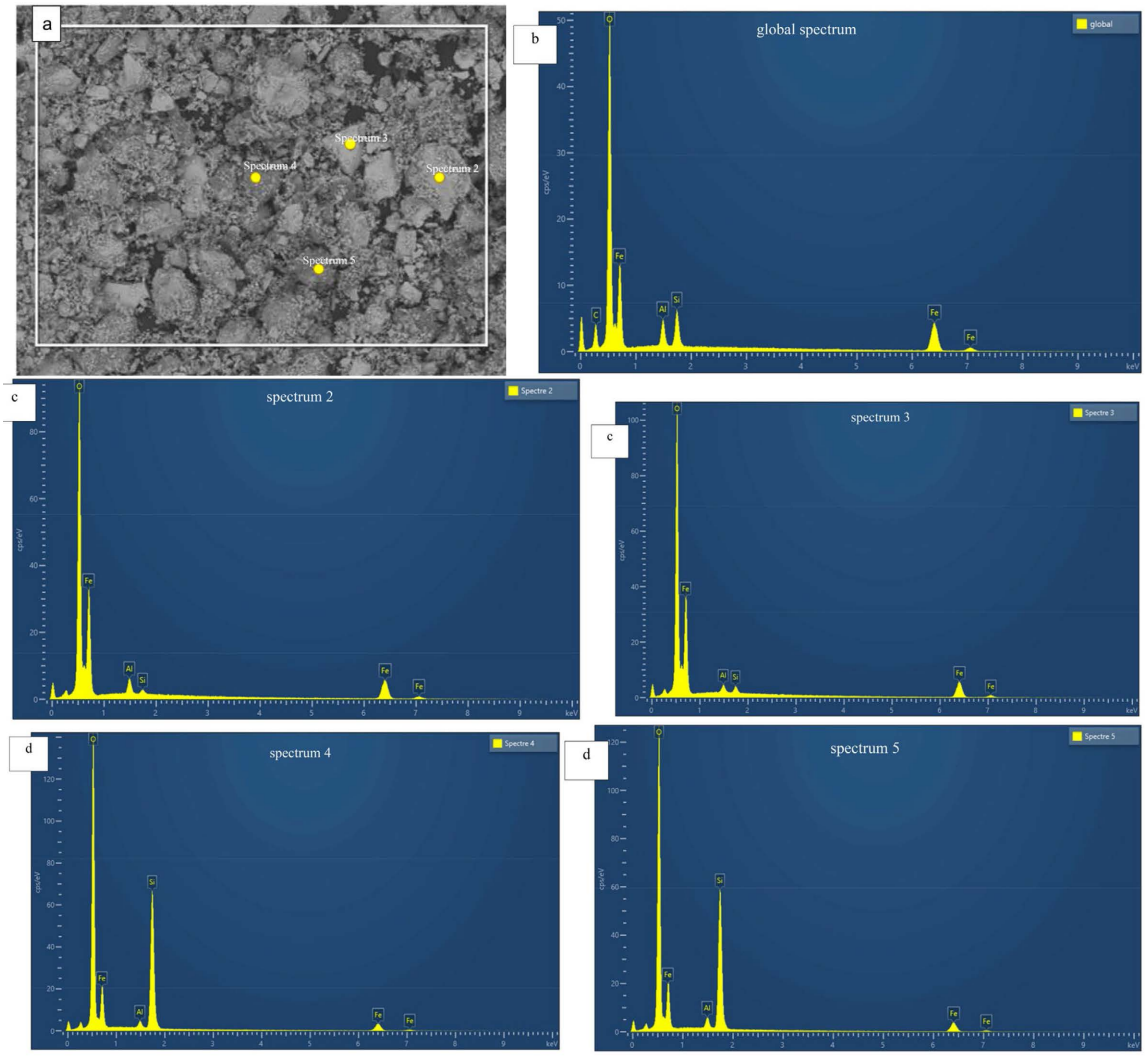

Figure 6. EDX quantitative analyses of Bandjéli crude iron ore with SEM image (a), global spectrum of the hole area (b), hematite-rich grains local spectra (c), and quartz-rich grains local spectra (d).

3.5. Comparison between XRF and EDX Results

XRF performs quantitative measurements across the entire analyzed volume, using X-ray excitation to identify and measure elements at depth, regardless of the sample surface. This technique offers excellent reproducibility for major and trace elements in solid matrices in geology and metallurgy. In contrast, EDX, usually coupled with scanning electron microscopy (SEM), performs essentially qualitative/semi-quantitative analysis, targeting specific microzones or grains of the sample, by probing down to about 1 μm below the surface. EDX results are therefore sensitive to local heterogeneity, surface condition (relief, roughness, coating), and the thickness of the analyzed layer, which may explain the slight overestimation of silica and underestimation of alumina compared to XRF data.

3.6. Analysis by Fourier Transform Infrared Spectroscopy

The IR spectrum shown in **Figure 7** reveals a mineral composition dominated by

hematite, identifiable in particular by striking peaks between 470 and 5218 cm^{-1}, attributed to the Eu and A2u vibrational modes typical of this iron mineral [13] [14]. The presence of silica is highlighted by intense bands located between 1000 and 1100 cm^{-1}, corresponding to the asymmetric elongation vibrations of Si-O-Si [14], as well as by peaks around 790 cm^{-1} attributed to the symmetric vibrations of silica [15]. The superposition of signals in the 1000 - 600 cm^{-1} zone reflects the coexistence of the dominant mineral phases (hematite), as well as the accessory silica. This spectrum is thus consistent with the chemical composition of the ore, which is rich in hematite with moderate proportions of silica.

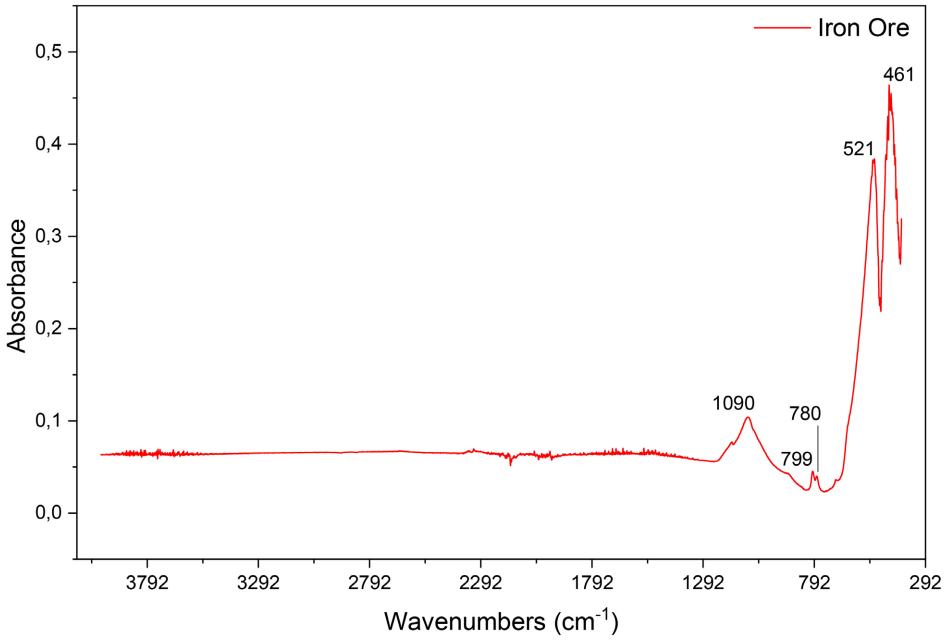

Figure 7. IR spectrum of Bandjéli crude iron ore.

4. Conclusion

This study makes an essential contribution to our knowledge of Bandjéli iron ore, providing for the first time a modern mineralogical and chemical characterization, based on a full range of analytical techniques. The results reveal the very high purity of the ore, as well as a low presence of gangue minerals and undesirable elements, demonstrating its strong potential for metallurgical and industrial applications. The high hematite content of the Bandjéli ore allows for efficient mineralization, leading to the generation of ferric ions, which can be used in acidic aqueous solutions with hydrogen peroxide to form the Fenton reagent. Under UV irradiation, this reagent enables an effective photo-Fenton reaction for the degradation of recalcitrant organic pollutants. This process offers an environmentally friendly and efficient method for wastewater treatment. Furthermore, the conversion of hematite into a high-purity magnetic oxide at a temperature below 570˚C in the presence of hydrogen allows the synthesis of a magnetically recoverable photocatalyst (e.g. co-precipitated with ZnO), facilitating easy separation after

treatment, a major challenge for the large-scale industrial application of photocatalysts. This naturally occurring, inexpensive, and readily available magnetic material overcomes the limitations of expensive supports such as porous glass or rings, which often reduce photocatalytic efficiency. These results encourage the conduct of pilot-scale catalytic tests, as well as economic feasibility studies for the sustainable and viable industrial implementation of these innovative processes for wastewater treatment. This approach fills an important gap in contemporary scientific literature, and provides a reliable database for the development of new processes, the optimization of deposit beneficiation and the implementation of more environmentally-friendly practices. This work paves the way for in-depth research in materials chemistry and encourages more sustainable and efficient management of Togolese mineral resources, thus contributing to the scientific and economic enhancement of the Bandjéli site within the African and international industrial landscape.

Acknowledgements

The authors would like to thank the technical staff from the Laboratory of Automation, Process Engineering, and Pharmaceutical Engineering (LAGEPP), Dr. Yves CHEVALIER from LAGEPP for his constant availability, the Analytical Chemistry Laboratory from Electronic Physic and Chemistry (CPE) high school of Lyon for the XRF analysis, and the Waste Management, Treatment and Recovery Laboratory (GTVD) from University of Lomé in Togo.

The authors would also like to thank the Cooperation and Cultural Action Service (SCAC) of the French Embassy in Togo for their financial support of this work through excellence grant awarded.

Conflicts of Interest

The authors declare no conflicts of interest regarding the publication of this paper.

References

[1] Mahadik, M.A., An, G.W., David, S., Choi, S.H., Cho, M. and Jang, J.S. (2017) Fabrication of A/R-TiO_2 Composite for Enhanced Photoelectrochemical Performance: Solar Hydrogen Generation and Dye Degradation. *Applied Surface Science*, **426**, 833-843. https://doi.org/10.1016/j.apsusc.2017.07.179

[2] Souza, A.H.D., Krüger, F.L.V., Araújo, F.G.D.S. and Mendes, J.J. (2021) Mineralogical Characterization Applied to Iron Ore Tailings from the Desliming Stage with Emphasis on Quantitative Electron Microscopy (QEM). *Materials Research*, **24**, e20190677. https://doi.org/10.1590/1980-5373-mr-2019-0677

[3] Wang, C., Jing, J., Qi, Y., Zhou, Y., Zhang, K., Zheng, Y., *et al.* (2023) Basic Characteristics and Environmental Impact of Iron Ore Tailings. *Frontiers in Earth Science*, **11**, Article 1181984. https://doi.org/10.3389/feart.2023.1181984

[4] Bendaikha, W., Larbi, S. and Ramdane, A. (2024) Mineralogical and Chemical Characterization of an Oolitic Iron Ore, and Sustainable Phosphorus Removal. *Journal of the Southern African Institute of Mining and Metallurgy*, **124**, 59-66. https://doi.org/10.17159/2411-9717/2051/2024

[5] Chebel, N., Nettour, D., Chettibi, M., Chaib, R., Khoshdast, H. and Hassanzadeh, A. (2024) Studying on Mineralogical and Petrological Characteristics of Gara Djebilet Oolitic Iron Ore, Tindouf (Algeria). *Physicochemical Problems of Mineral Processing*, **59**, Article 178382. https://doi.org/10.37190/ppmp/178382

[6] Mahanta, C., Sahoo, P., Mohanta, M., Rath, R., Dey, S., Tripathy, S., *et al.* (2023) Mineralogical Characteristics of Hematitic Iron Ore: A Geometallurgical Study on Ore from Eastern India. *Minerals*, **13**, Article 1194. https://doi.org/10.3390/min13091194

[7] Patra, S., Pattanaik, A., Venkatesh, A.S. and Venugopal, R. (2019) Mineralogical and Chemical Characterization of Low Grade Iron Ore Fines from Barsua Area, Eastern India with Implications on Beneficiation and Waste Utilization. *Journal of the Geological Society of India*, **93**, 443-454. https://doi.org/10.1007/s12594-019-1199-4

[8] Muwanguzi, A.J.B., Karasev, A.V., Byaruhanga, J.K. and Jönsson, P.G. (2012) Characterization of Chemical Composition and Microstructure of Natural Iron Ore from Muko Deposits. *ISRN Materials Science*, **2012**, 1-9. https://doi.org/10.5402/2012/174803

[9] de Barros, P.L., Iles, L., Frame, L.D. and Killick, D. (2020) The Early Iron Metallurgy of Bassar, Togo: Furnaces, Metallurgical Remains and Iron Objects. *Azania*: *Archaeological Research in Africa*, **55**, 3-43. https://doi.org/10.1080/0067270x.2020.1721841

[10] Robion-Brunner, C., Coustures, M., Dugast, S., Tchetre-Gbandi, A. and Béziat, D. (2022) Origines et étapes de la diversité des techniques sidérurgiques en Afrique de l'Ouest: Le cas de la production du fer en pays bassar (nord du Togo) du XIIIe au XXe siècles. *Afriques*, **13**, 1-64.

[11] Toi Bissang, B., Aragón-Barroso, A.J., Baba, G., González-López, J. and Osorio, F. (2024) Integrated Assessment of Heavy Metal Pollution and Human Health Risks in Waters from a Former Iron Mining Site: A Case Study of the Canton of Bangeli, Togo. *Water*, **16**, Article 471. https://doi.org/10.3390/w16030471

[12] Huang, F., Liu, H., Wang, H., Sun, F., Chen, T., Chen, D., *et al.* (2020) The Activation of Hematite for the Catalytic Hydrogen Peroxide Degradation of Methylene Blue. *Desalination and Water Treatment*, **201**, 383-392. https://doi.org/10.5004/dwt.2020.26003

[13] Jubb, A.M. and Allen, H.C. (2010) Vibrational Spectroscopic Characterization of Hematite, Maghemite, and Magnetite Thin Films Produced by Vapor Deposition. *ACS Applied Materials & Interfaces*, **2**, 2804-2812. https://doi.org/10.1021/am1004943

[14] Šuligoj, A., Grinberg, D. and Paz, Y. (2021) Post-Excitation Transient IR Phenomena in A-Fe_2O_3 Films. *The Journal of Physical Chemistry C*, **125**, 28013-28024. https://doi.org/10.1021/acs.jpcc.1c09118

[15] Ellerbrock, R., Stein, M. and Schaller, J. (2022) Comparing Amorphous Silica, Short-Range-Ordered Silicates and Silicic Acid Species by FTIR. *Scientific Reports*, **12**, Article No. 11708. https://doi.org/10.1038/s41598-022-15882-4